

Unidirectional behavior of uncompensated Fe orbital moments in exchange-biased Co/FeMn/Cu(001)

D. Schmitz,^{*} E. Schierle, N. Darowski, H. Maletta, and E. Weschke
Helmholtz-Zentrum Berlin für Materialien und Energie, Albert-Einstein-Straße 15, D-12489 Berlin, Germany

M. Gruyters
Institut für Experimentelle und Angewandte Physik, Christian-Albrechts-Universität zu Kiel, D-24098 Kiel, Germany
 (Received 8 August 2008; revised manuscript received 20 April 2010; published 15 June 2010)

Exchange-bias and uncompensated magnetic moments in epitaxially grown fcc Co/FeMn/Cu (001) are studied with element-specific x-ray magnetic circular dichroism. The magnitude of the uncompensated Fe moments of the antiferromagnet FeMn and the sign of their magnetic coupling to the ferromagnet Co are indicated by the circular dichroism signal. In the biased state the orbital-to-spin-moment ratio of the uncompensated Fe moments is found to be enhanced in remanence after magnetizing into the field cooling direction but zero after magnetizing into the opposite direction. This unidirectional behavior is mainly caused by a change in the orbital moment component along the easy magnetization axis probed in the experiment. It clearly reflects the macroscopic unidirectional loop shift being characteristic for the exchange-bias effect. This result suggests that spin-orbit coupling between rotatable spin and pinned orbital moments belongs to the magnetic interactions which cause the exchange-bias effect in the present system.

DOI: [10.1103/PhysRevB.81.224422](https://doi.org/10.1103/PhysRevB.81.224422)

PACS number(s): 75.70.Cn, 75.30.Et, 75.30.Gw

I. INTRODUCTION

Exchange bias occurs in systems where a ferromagnet (FM) and an antiferromagnet (AFM) are in contact. One feature of this effect is that the hysteresis loop is displaced from zero along the magnetic field axis. It was first observed in 1956 for fine particles of cobalt with a cobaltous oxide shell.¹ One year later its origin has been postulated as being the exchange interaction between the spins of the atoms in the cobalt and the ions in the cobalt oxide.²

Per definition, spins of one antiferromagnetic sublattice are called “uncompensated” if moments of the other antiferromagnetic sublattice, oriented into the opposite direction and therefore usually compensating the moment from the first sublattice, are missing. If the magnetization direction of the FM is reversed, one part of the uncompensated moments of the AFM follows because the coupling to the FM dominates. Another part of the uncompensated moments does not reverse with the FM because the coupling to the AFM dominates. The latter part is the so-called “pinned fraction” of uncompensated moments which has been supposed to be crucial for exchange bias.³

For samples where the ferromagnetic and antiferromagnetic layers consist of different chemical elements it is possible to separate the small contribution of uncompensated AFM moments from the dominant contribution of FM moments by element-specific x-ray magnetic dichroism methods. This has been utilized in several recent experimental studies. The spin structure at the interface of exchange-biased Co/FeMn was studied comparing x-ray magnetic circular dichroism (XMCD) spectra which were measured reversing the magnetization either by an external field or by rotating the sample.⁴ Strong ferromagnetic and 90° coupling between two Co layers separated by an FeMn spacer were reported for different spacer thicknesses.⁵ The correlation between exchange-bias and pinned interfacial spins in systems

which are relevant for applications was investigated comparing element-specific hysteresis loops for sample rotations where the magnetic cooling field direction was parallel or antiparallel to the polarization vector of the radiation.³ The depth profile of uncompensated spins in Co/FeF₂ was determined by combining x-ray resonant magnetic reflectometry (XRMR), polarized neutron reflectometry, and micromagnetic simulations.⁶ Parallel versus antiparallel interfacial coupling in Co/FeF₂ was investigated by combining x-ray magnetic linear dichroism with XMCD spectra and hysteresis loops.⁷ Different magnetic coupling mechanisms with different coupling signs between uncompensated Co moments in amorphous CoO and Fe moments were identified by variation in the Cu spacer thickness and temperature⁸ partly explaining the earlier finding that there is no simple quantitative relation between the number of pinned uncompensated spins and the exchange-bias field in this particular system.⁹ The depth profiles of rotatable and pinned uncompensated Mn moments in Fe/MnPd were determined using XRMR.¹⁰

In order to study the interplay between the exchange-bias field and the uncompensated moments at the interface to the FM we combined element-specific hysteresis loops with XMCD spectroscopy. Using the excellent results regarding growth, structure and magnetism of fcc Co/FeMn bilayers obtained in Refs. 11–14 as a starting point we prepared epitaxially grown ferromagnetic Co (5 atomic layers thick) on antiferromagnetic FeMn (12 atomic layers thick) on Cu(001). We studied this system at low sample temperatures (down to 5 K) in combination with moderate magnetic fields (up to 10 kOe) to account for the relatively large coercive fields observed after field cooling to low sample temperatures. Field cooling through the Néel temperature of the FeMn was feasible because the Néel temperature could be reduced from the bulk value of 490 K (Ref. 15) (at which the structure of the sample would be destroyed by interdiffusion) to 380 K by choosing an appropriate FeMn thickness of 12 atomic layers.^{12,16}

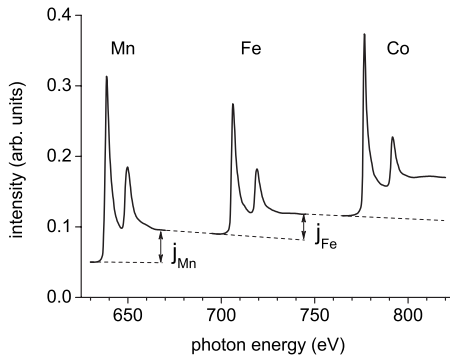


FIG. 1. X-ray absorption overview spectra of Co/FeMn measured after Co deposition across the $L_{2,3}$ edges of Mn, Fe, and Co. The edge jumps of Mn and Fe are schematically indicated as j_{Mn} and j_{Fe} , respectively.

In order to separate the small ferromagnetic signal of the uncompensated moments in the AFM (FeMn) from the dominating one of the FM (Co) the element-specific methods XMCD and XRMR have been employed. XMCD with total electron yield detection has been used to determine ferromagnetically ordered magnetic moments and XRMR as a photon-in-photon-out technique to measure the hysteresis loops. These methods require to tune the photon energy to and to scan it—in the present case—across the $L_{2,3}$ absorption edges of the $3d$ elements involved. In addition, elliptically polarized electromagnetic radiation with a high degree of circular polarization is required to utilize the circular dichroism effect. Moreover, for the comparison of the tiny circular dichroism effects in different magnetization states of the sample it is essential to measure the XMCD spectra with good statistics and to reverse the helicity of the elliptically polarized radiation with high precision.

II. SAMPLE PREPARATION AND EXPERIMENTAL SETUP

The samples were prepared in an experimental station which had been designed for *in situ* preparation and XMCD measurements of magnetic thin films in remanence under ultrahigh-vacuum conditions. As the substrate a Cu(001) single crystal was used which had carefully been cleaned by sputtering and annealing cycles as verified with Auger electron spectroscopy and low-energy electron diffraction (LEED). The base pressure of the preparation chamber was 2×10^{-10} mbar. The pressure typically increased to 2×10^{-9} mbar during the codeposition of Mn and Fe and to 7×10^{-10} mbar during the deposition of Co using commercial electron-beam evaporators. The films were deposited at room temperature with a rate of about $0.5 \text{ \AA}/\text{min}$ for each chemical element. For the deposition of the FeMn, the Fe and Mn evaporators were operated at equal rates. The individual rates of the evaporators were calibrated using a quartz oscillator. The thicknesses of the deposited films were achieved based on these rates using appropriate deposition times. The Fe concentration in the FeMn was checked with x-ray absorption spectroscopy using the overview spectrum shown in Fig. 1 which was measured after Co deposition.

The edge jumps j_{Mn} and j_{Fe} schematically indicated in Fig. 1 were corrected for the different photoabsorption cross sections.¹⁷ The corrected edge jumps \hat{j}_{Mn} and \hat{j}_{Fe} were then used to determine the Fe concentration $\hat{j}_{\text{Fe}}/(\hat{j}_{\text{Mn}} + \hat{j}_{\text{Fe}})$. In this way an Fe concentration of 44% was determined for the present sample which is close to the aspired value of 50% and well within the range from 25% to 55% for which the fcc structure is the most stable one.¹⁶ Changing the Fe concentration from 50% to 44% increases the Néel temperature of a 12 atomic layers thick FeMn film from 380 to 395 K.¹² After Co deposition the quality of the film was checked with LEED, and bright and sharp diffraction spots as for the bare Cu substrate were observed. Finally the sample was capped with 30 \AA Pt and checked again with XMCD before it was exposed to air during the transfer to the high-field end station where it was measured as described below. The high-field end station has been designed for XMCD and XRMR measurements in high magnetic fields (up to 7 T) and low sample temperatures (down to 5 K) under ultrahigh-vacuum conditions (pressure 10^{-10} mbar). It is permanently installed at the UE46-PGM/1 beamline at the electron storage ring BESSY II of the Helmholtz Centre Berlin.

III. RESULTS AND DISCUSSION

XMCD spectra were measured in fixed magnetization states of the samples by reversing the helicity of the synchrotron radiation after a complete energy scan. This procedure is equivalent to rotating the sample such that the in-plane component of the magnetization reverses its direction relative to the polarization vector as described in Refs. 3 and 4. Magnetizing after deposition creates a well-defined state of the magnetization of the FM, and field cooling aligns the moments of the AFM and activates the exchange bias. Reversing the magnetization after field cooling reverses rotatable uncompensated spins whereas the pinned fraction keeps the initial magnetization direction. Reversing the magnetization a second time or more serves to test whether the initial reversal behavior is maintained or training effects occur.

Hysteresis loops were measured in reflection using an angle of incidence of 30° with respect to the sample surface and tuning the photon energy to the L_3 absorption maximum. Under these conditions the amplitudes of the circular dichroism in both, absorption and reflection, exhibit an extremal value as a function of photon energy. The external magnetic field was applied along the easy magnetization axis of the Co film which (below the Néel temperature of the FeMn film) is along an in-plane $\langle 100 \rangle$ direction.¹³

Element-specific hysteresis loops are shown in Fig. 2 for Co (dashed line) and Fe (solid line) at 5 K after field cooling. As the ordinate the asymmetry is shown which is defined as the difference of two measurements with opposite photon helicities divided by the sum of the two. Sensitivity to one of the chemical elements was obtained by tuning the photon energy to the corresponding L_3 absorption edge. The sign of the asymmetry is the same for Co and Fe, indicating together with the corresponding circular dichroism spectra (not shown) that the magnetic moments of Fe and Co are oriented parallel to each other.

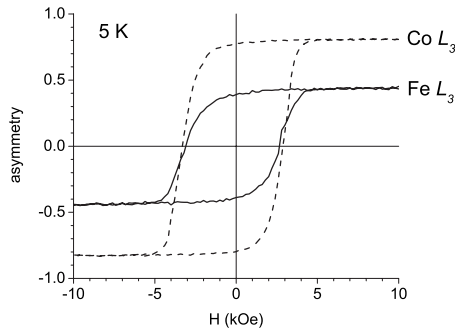


FIG. 2. Hysteresis loops of Co/FeMn measured at Co L_3 (dashed line) and Fe L_3 (solid line) in reflection at a temperature of 5 K after field cooling in an external magnetic field of 5 kOe.

A significant pinned fraction of uncompensated Fe moments in the AFM would result in a vertical shift of the corresponding hysteresis loops because the pinned moments would be oriented parallel to the rotatable moments for magnetization into the field cooling direction but antiparallel for magnetization into the opposite direction. Such a vertical shift of the hysteresis loops is very small under the experimental conditions used even after field cooling to 5 K. The corresponding pinned fraction of uncompensated Fe moments of the AFM can be estimated to be at most 2%. This small fraction qualitatively agrees with the relatively small exchange-bias field of at most 200 Oe as compared to the coercive field of 3000 Oe.

The hysteresis loops of Co after field cooling to 5 K in an external magnetic field of 5 kOe are shown in Fig. 3 as a function of temperature between 5 K (top panel) and 300 K

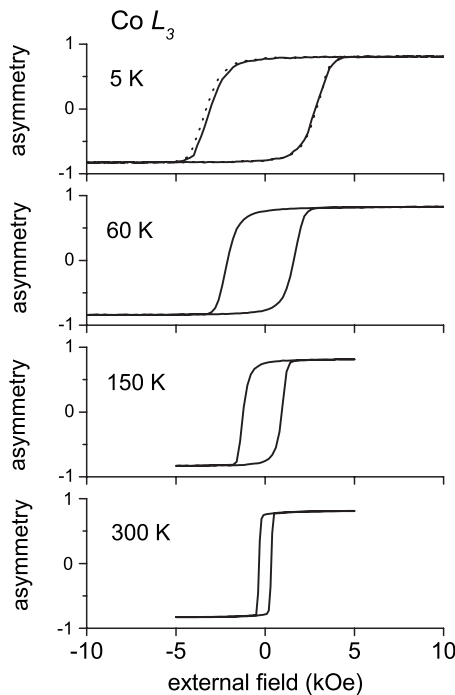


FIG. 3. Hysteresis loops of Co/FeMn measured at Co L_3 in reflection at different temperatures (values indicated in the figure) after field cooling to 5 K. The dotted curve in the top panel was measured directly after field cooling, the solid curves after training.

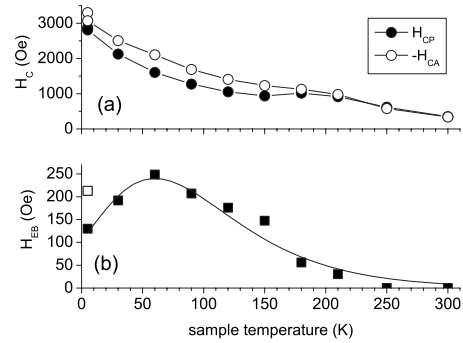


FIG. 4. Coercive fields (a) on the descending (open circles) and ascending branches (full circles) of the Co hysteresis loops shown in Fig. 3 and corresponding exchange-bias fields (b) as a function of sample temperature. After field cooling to 5 K the exchange-bias field decreases from 210 Oe (open square) to 130 Oe (solid square) by training.

(bottom panel). The coercive fields of up to several kilo-Oersted are much larger than the exchange-bias fields and decrease with increasing sample temperature. The corresponding values of the coercive fields parallel (antiparallel) to the cooling field $H_{CP} > 0$ ($H_{CA} < 0$) were used to calculate the values of the exchange-bias field $H_{EB} = -(H_{CP} + H_{CA})/2$ and are shown in Fig. 4. Directly after field cooling an exchange-bias field of about 200 Oe is observed at 5 K. After several hysteresis loops at 5 K H_{EB} saturates at 130 Oe, i.e., a training effect is observed. At 5 K the average coercive field $H_C = (H_{CP} - H_{CA})/2$ is nine times larger than at 300 K, and between 50 and 150 K it is seven times larger than H_{EB} . These values indicate that the hysteresis loops of the present system are dominated by the anisotropy of the AFM. For increasing temperature H_{EB} decreases to 0 Oe at about 300 K. Below this temperature a local maximum appears in $-H_{CA}$ and also but less pronounced in H_{CP} as frequently observed for exchange-bias systems.¹⁵

Figure 5 shows the absorption and circular dichroism spectra of Fe at a sample temperature of (a) 5 and (b) 300 K measured in the total electron yield. For each temperature two dichroism spectra are shown which were measured after field cooling in remanence. The relative amplitudes of the circular dichroism without subtracting the background under the absorption spectra are tiny, i.e., typically 1% or smaller at the L_3 resonance, explaining the limited statistical quality of the dichroism spectra. Nevertheless, it is clearly resolved that the relative dichroism amplitudes decrease with increasing temperature, and that the spectral shape of the circular dichroism of Fe strongly changes between the two branches of the hysteresis loops. In the circular dichroism spectra the L_3/L_2 intensity ratio is much larger on the descending branch (black line), i.e., for remanent magnetization parallel to the field cooling direction, than on the ascending branch (gray line), i.e., for remanent magnetization antiparallel to the field cooling direction. This unidirectional behavior of the spectral shape reflects the unidirectional nature of the exchange-bias effect. It can neither be explained by uncompensated Fe total moments which solely change their orientation by 180° nor by a significant pinned fraction. In both cases circular dichroism spectra with different amplitudes but similar spectral

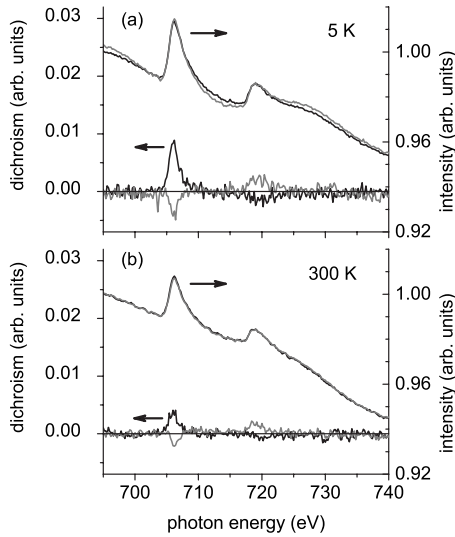


FIG. 5. Absorption and circular dichroism spectra of Fe measured after field cooling to 5 K at sample temperatures of (a) 5 K and (b) 300 K on the descending (black lines) and ascending branches (gray lines) of the hysteresis loops.

shapes would be observed. Instead it can be explained by a strongly changing orbital-to-spin-moment ratio of the uncompensated Fe moments. This is demonstrated in Fig. 6 where the two dichroism spectra from Fig. 5(a) are compared with the ones of 5 atomic layers Fe on V(110) which serve as

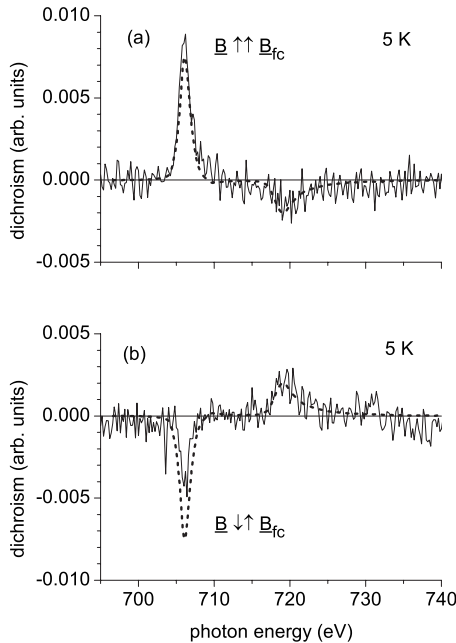


FIG. 6. Circular dichroism spectra of Fe at 5 K from Fig. 5(a) (solid lines) for remanent magnetization on the (a) descending and (b) ascending branches of the hysteresis loops. For comparison the ones of 5 atomic layers Fe on V(110) (dashes lines) from Ref. 18 which serve as reference spectra are also shown. The shape of the circular dichroism spectra strongly changes between the two branches. The L_3/L_2 circular dichroism intensity ratio, and thus the orbital-to-spin-moment ratio, is much larger on the descending than on the ascending branch.

reference spectra.¹⁸ The reference spectra which only differ in sign between Figs. 6(a) and 6(b), respectively, have been scaled such that they coincide with the other spectra at L_2 . On the descending branch of the hysteresis loops [Fig. 6(a)] the area at L_3 is considerably increased with respect to the reference spectrum. According to the magneto-optical sum rules for the circular dichroism¹⁹ such a spectral shape indicates that the orbital-to-spin-moment ratio is increased as compared to the reference. Contrary, on the ascending branch of the hysteresis loops [Fig. 6(b)] the area at L_3 is considerably decreased such that it is similar to the area at L_2 . According to the sum rules¹⁹ this spectral shape indicates that the orbital moment vanishes along the direction probed in the experiment. Consequently, an unidirectional behavior of the orbital-to-spin-moment ratio is observed. In addition, the similarity of the absorption spectra and the areas under the circular dichroism signals indicate that the sums of spin moment and the magnetic dipole moment for both magnetization directions are similar within the experimental uncertainty. Therefore finally the orbital moment displays the unidirectional nature of the exchange-bias effect. This is the main result of the present paper which is discussed in more detail below.

Before turning to this discussion we address the number of the uncompensated Fe moments by taking into account the Fe asymmetry after background subtraction. After correcting for the incomplete degree of circular polarization and the angle of incidence, these asymmetries at the Fe L_3 maximum are 18% (9%) at 5 K and 11% (5%) at 300 K for remanent magnetization parallel (antiparallel) to the field cooling direction. A precise determination of the amount of uncompensated Fe moments based on the asymmetry is not possible because as described above the L_3/L_2 dichroism intensity ratio of the present system is different as compared to the one of the reference. It is just as little possible to sincerely determine the average Fe magnetic moments using the sum rules because the small signal-to-background ratios in the absorption spectra (Fig. 5) cause large experimental uncertainties, in particular, for the areas between the absorption spectra and the step functions which appear in the denominator of the sum rules for the spin and orbital moments. As already stated above, it is solely possible to conclude by comparing the absorption and dichroism spectra that only the orbital moments but not the sums of spin and magnetic dipole moment significantly change between both magnetization directions. Moreover, it is very reasonable to assume that the uncompensated Fe moments are located in the upper part of the FeMn film close to the ferromagnetic layer where direct exchange interaction with the Co moments can occur. XMCD measurements in absorption with total electron yield detection are particularly sensitive to uncompensated moments located in the upper part of the FeMn film. This is the case because the mean-free path of the secondary photoelectrons is about 2 nm so that the signal from the uppermost FeMn layer is about three times larger than the one from the downmost layer of the 2.2-nm-thick FeMn film. These aspects must be considered when comparing the observed asymmetries with the value of 28% for bulk Fe.²⁰

Returning to the main result of the present paper, the unidirectional behavior of the orbital moment is discussed in the

following. For remanent magnetization *parallel* to the field cooling direction the orbital moment is significantly enhanced. One possible mechanism has been described in a band picture by Eriksson *et al.*²¹ They have explained for Fe, Co, and Ni in the fcc structure how a changing band filling influences the size of the orbital moment. In Co and Fe the majority band gives nearly no contribution to the orbital moment because it is nearly completely filled. Therefore the orbital moments of Co and Fe are mainly due to the minority electrons. Those give a positive contribution to the total orbital moment because the minority band is more than half filled and because the minority states with positive (negative) magnetic quantum numbers are pushed down (up) due to spin-orbit interaction. For the same reasons the positive orbital contribution increases if the minority band is emptied. Therefore a charge transfer away from Fe can explain an increased orbital moment. Moreover, in a rigid-band picture modifying the band filling also means that the levels which are located near the Fermi energy change. Consequently the energy differences between levels located just above and below the Fermi energy and therefore, according to second-order perturbation theory, the spin-orbit coupling energy and finally the magnetocrystalline anisotropy change.²²

For remanent magnetization *antiparallel* to the field cooling direction a small orbital-to-spin-moment ratio with a value close to zero is observed. There are two possible explanations for this observation. Either the orbital moment is large but mainly oriented perpendicular to the direction, say [100], probed in the present experiment or its absolute value is small. The measured spectra demonstrate that the areas under the Fe absorption spectra (see Fig. 5) which are a measure for the number of 3*d* holes¹⁹ do not depend on the magnetization direction. Therefore in the band picture described above the charge transfer away from Fe would not depend on the magnetization direction, suggesting that the absolute value of the Fe orbital moment does not depend on the magnetization direction. Therefore for magnetization antiparallel to the field cooling direction the orbital moment could be oriented perpendicular to the direction probed in the present XMCD experiment. That could be the result of com-

peting spin-orbit and crystal-field interactions leading to frustrated orbital moments. Indeed, an out-of-plane magnetocrystalline anisotropy at the Co/FeMn interface is supported by the calculations of Nakamura *et al.*²³ The corresponding orbital moments could be located on terraces of the surface of a 3*Q*-like antiferromagnetic spin structure because there they are not compensated out of plane.²⁴ The orbital moment could also be oriented in plane along the [010] or [0 $\bar{1}$ 0] direction which would be an easy magnetization direction and also perpendicular to the [100] direction probed in the experiment. These orbital moments could be located at monatomic steps on the surface of a 3*Q*-like antiferromagnetic spin structure because there they are not compensated in plane.²⁴ In order to determine the out-of-plane and in-plane directions of the orbital moment, XMCD measurements have to be performed after field cooling at different angles of incidence and azimuth angles, respectively.

Summarizing, we found that the uncompensated Fe orbital moments in Co/FeMn show a strongly unidirectional behavior in the biased state. For remanent magnetization parallel to the field cooling direction they are significantly larger than in the reference system Fe/V. For remanent magnetization antiparallel to the field cooling direction their component along this direction vanishes. This unidirectional behavior of a microscopic property clearly reflects the macroscopic unidirectional loop shift being characteristic for the exchange-bias effect. Therefore we suggest that besides the exchange interaction between rotatable and pinned uncompensated spin moments also the spin-orbit coupling belongs to the magnetic interactions which cause the exchange-bias effect in the present Co/FeMn system. This spin-orbit interaction acts between uncompensated spin moments which rotate with the ferromagnet and orbital moments which are pinned by the anisotropy of the antiferromagnet.

ACKNOWLEDGMENTS

Fruitful discussions with H. A. Dürr and F. Radu and technical support by S. Miemietz, S. Rudorff, and K. Effland is gratefully acknowledged.

*Corresponding author; schmitz@helmholtz-berlin.de

¹W. H. Meiklejohn and C. P. Bean, *Phys. Rev.* **102**, 1413 (1956).

²W. H. Meiklejohn and C. P. Bean, *Phys. Rev.* **105**, 904 (1957).

³H. Ohldag, A. Scholl, F. Nolting, E. Arenholz, S. Maat, A. T. Young, M. Carey, and J. Stöhr, *Phys. Rev. Lett.* **91**, 017203 (2003).

⁴W. J. Antel, Jr., F. Perjeru, and G. R. Harp, *Phys. Rev. Lett.* **83**, 1439 (1999).

⁵F. Matthes, A. Rzhetskii, L.-N. Tong, L. Malkinski, Z. Celinski, and C. M. Schneider, *J. Appl. Phys.* **93**, 6504 (2003).

⁶S. Roy, M. R. Fitzsimmons, S. Park, M. Dorn, O. Petravic, I. V. Roshchin, Z.-P. Li, X. Battle, R. Morales, A. Misra, X. Zhang, K. Chesnel, J. B. Kortright, S. K. Sinha, and I. K. Schuller, *Phys. Rev. Lett.* **95**, 047201 (2005).

⁷H. Ohldag, H. Shi, E. Arenholz, J. Stöhr, and D. Lederman,

Phys. Rev. Lett. **96**, 027203 (2006).

⁸M. Gruyters and D. Schmitz, *Phys. Rev. Lett.* **100**, 077205 (2008).

⁹M. Gruyters, *Phys. Rev. Lett.* **95**, 077204 (2005).

¹⁰S. Brück, G. Schütz, E. Goering, X. Ji, and K. M. Krishnan, *Phys. Rev. Lett.* **101**, 126402 (2008).

¹¹W. Kuch, F. Offi, L. I. Chelaru, M. Kotsugi, K. Fukumoto, and J. Kirschner, *Phys. Rev. B* **65**, 140408(R) (2002).

¹²F. Offi, W. Kuch, and J. Kirschner, *Phys. Rev. B* **66**, 064419 (2002).

¹³F. Offi, W. Kuch, L. I. Chelaru, K. Fukumoto, M. Kotsugi, and J. Kirschner, *Phys. Rev. B* **67**, 094419 (2003).

¹⁴W. Kuch, F. Offi, L. I. Chelaru, J. Wang, K. Fukumoto, M. Kotsugi, J. Kirschner, and J. Kunes, *Phys. Rev. B* **75**, 224406 (2007).

- ¹⁵J. Nogués and I. K. Schuller, *J. Magn. Magn. Mater.* **192**, 203 (1999).
- ¹⁶J. Seifert, T. Bernhard, M. Gruyters, and H. Winter, *Phys. Rev. B* **76**, 224405 (2007).
- ¹⁷B. L. Henke, E. M. Gullikson, and J. C. Davis, *At. Data Nucl. Data Tables* **54**, 181 (1993).
- ¹⁸D. Schmitz, J. Hauschild, P. Imperia, Y. T. Liu, and H. Maletta, *J. Magn. Magn. Mater.* **269**, 89 (2004).
- ¹⁹B. T. Thole, P. Carra, F. Sette, and G. van der Laan, *Phys. Rev. Lett.* **68**, 1943 (1992); P. Carra, B. T. Thole, M. Altarelli, and X. Wang, *ibid.* **70**, 694 (1993).
- ²⁰C. T. Chen, Y. U. Idzerda, H.-J. Lin, N. V. Smith, G. Meigs, E. Chaban, G. H. Ho, E. Pellegrin, and F. Sette, *Phys. Rev. Lett.* **75**, 152 (1995).
- ²¹O. Eriksson, B. Johansson, R. C. Albers, A. M. Boring, and M. S. S. Brooks, *Phys. Rev. B* **42**, 2707 (1990).
- ²²P. Bruno, *Phys. Rev. B* **39**, 865 (1989).
- ²³K. Nakamura, T. Ito, and A. J. Freeman, *Phys. Rev. B* **70**, 060404(R) (2004).
- ²⁴K. Lenz, S. Zander, and W. Kuch, *Phys. Rev. Lett.* **98**, 237201 (2007).